Thesis for the Degree of Licentiate of Engineering

Slot Array Antennas at V-band based on Inverted Microstrip Gap Waveguide

Jinlin Liu

CHALMERS

Department of Signals and Systems
Chalmers University of Technology

Göteborg, Sweden 2017

Slot Array Antennas at V-band based on Inverted Microstrip Gap Waveguide

Jinlin Liu

Technical report number: 2017/2017
ISSN 1403-266X

Department of Signals and Systems
Division of Communications and Antenna Systems
Chalmers University of Technology
SE–412 96 Göteborg
Sweden
Telephone: +46 (0)31 – 772 1000
Email: jinlin.liu@chalmers.se

Typeset by the author using LaTeX.

Chalmers Reproservice
Göteborg, Sweden 2017

To my family

"Look deep into nature, and then you will understand everything better"
-Albert Einstein

Abstract

Recently, gap waveguide technology is introduced as a proper guiding structure for millimeter-systems. The conception of gap waveguide technology can be modeled for theoretical analysis by two parallel plates, a top perfect electric conductor layer and a bottom perfect magnetic conductor layer. This structure stops all modes propagating in all directions except for a quasi-TEM mode when the gap between perfect electric conductor and perfect magnetic conductor plates is smaller than quarter wavelength at an operating frequency. Until now there are already four different visions of this novel concept—groove, ridge, inverted microstrip and microstrip ridge gap waveguides. Among those four structures, the inverted microstrip gap waveguide has some obvious advantages. First of all, it has a uniform bed of nails while the others do not. This uniform pin structure makes the fabrication much easier and cheaper. Secondly, fabrication of microstrip circuitry on PCB by etching is accurate and very low cost. In addition, theories and design principles of microstrip technologies are very well-developed. Therefore, my work in this Lic. thesis is focusing on the theory of inverted microstrip gap waveguide and its applications on millimeter wave array antenna design.

Keywords: metallic pins, perfect magnetic conductor, inverted microstrip gap waveguide, slots array and variational method.

Preface

This thesis is in partial fulfillment for the degree of Licentiate of Engineering at Chalmers University of Technology.

The work that has resulted in this thesis was carried out between September 2014 and April 2017 and has been performed within the Division of Antenna Systems at the Department of Signals and Systems, Chalmers University of Technology. Prof. Dr.Jian Yang has been the examiner and main supervisor, and Associate Prof. Ashraf Uz Zaman has been the co-supervisor.

This work is financially supported by the Swedish Governmental Agency for Innovation Systems VINNOVA via a project within the VINN Excellence center CHASE and the European Research Council (ERC) under 7th Framework Program ERC grant number 3222804.

Acknowledgments

First of all, the great appreciation and the thanks I would like to give to Prof.Dr.Per-Simon Kildal for his talented idea of gap waveguide structures. His leaving is irreversibly loss in the antenna world. Then I would like to thank Prof.Dr.Marianna Ivashina and Prof.Dr.Jian Yang for their kind guidance to work on challenging and relevant research topics. I also would like to thank my supervisor Assistant Prof.Dr.Ashraf Uz Zaman for his selection working in the group and kind supervision of the project. His knowledges in gap waveguide and array antennas I admire very much. I would like to express my appreciation to Associate Prof.Dr.Rob Maaskant and Assistant Prof.Dr.Andreas Alayon Glazunov for their encouragements in research and study in fields theory of guided waves and wireless communications during these years. In the end I thank to Prof.Dr.Eva Rajo-Iglesias for her time to come to my Lic. seminar.

Furthermore, I would like to appreciate every member in antenna group for the perfect research and work environment. First of all, I am very grateful for my officemate Abbas Vosoogh, who is not only a microwave and antenna scientist and engineer, but also an artist for his creative ideas and highly efficient work in the field of gap waveguide technology. It makes research simple and highly efficient to collaborate with him. Then I would like to thank Carlo Bencivenni for his kind help and encouragement in the group. He has instructed lots of knowledge about antenna array synthesis at the beginning and this is very benefit for the following work. Many thanks to Dr.Aidin Razavi for his helpful advices in research and study in the group. Then I am very grateful to Sadegh Mansouri Moghaddam for his kind discussion in antennas. Then I appreciate Dr.Astrid Algaba Brazalez for her many years hard work and promising achievements on the transition design of inverted microstrip gap waveguide. Then I would like to thank Madeleine Schilliger Kildal, Artem Roev, Oleg Iupikov, Parastoo Taghikhani, Navid Amani, Pegah Takook, Samar Hosseinzadegan, Tomas Rydholm and Cristina Rigato for their getting along with in the group. Many thanks to Markus Froehle for his helpful advices in the thesis. Then I would like to thank Dr.Xuezhi Zeng, Dr.Simon He, Dr.Wei Yang, Li Yan, Dr.Yixiao Yun, Chao Fang, Xinglin Zhang, Dr.Yinan Yu, Dr.Wanlu Sun, Prof.Dr.Xiaoming Chen, Prof.Dr.Kin Cheong Sou, Zhixing Chen, Dr.Yujiao Song, Xinxin Yang, Sining An, Dr.Lei Shi from Chinese Department of Aerospace, Dr.Bin Dong from Chinese

Institute of Academy and Dr. Fangfang Fan from Xidian University. In addition I also appreciate my Iranian friends Ali at Kerman University and Davoud at Kashan University for their unreserved discussions on array antennas.

My special thanks go to all the former and current colleagues of the Signals and Systems Department for creating a nice and enjoyable working environment. We've had a lot of fun and enjoyable moments both at work and afterwork time.

Jinlin Liu

List of Publications

This thesis is based on the work contained in the following appended papers:

Paper 1
J. L. Liu, A. Vosoogh, A. U. Zaman, and P. S. Kildal, "Design of a Cavity-backed Slot Array Unit Cell on Inverted Microstrip Gap Waveguide", in *International Symposium on Antennas and Propagation, ISAP 2015*, Hobart, Tasmania, Australia, November 9-12th, 2015.

Paper 2
J. L. Liu, A. U. Zaman, and P. S. Kildal, "Optimizing the numerical port for inverted microstrip gap waveguide in full-wave simulators", in *10th European Conference on Antennas and Propagation, EuCAP 2016*, Davos, Switzerland, April 10-15th, 2016.

Paper 3
J. L. Liu, A. U. Zaman, and P. S. Kildal, "Design of transition from WR-15 to inverted microstrip gap waveguide", in *Global Symposium on Millimetre-Wave Technology and Applications, GSMM 2016*, Espoo, Finland, June 6-8th, 2016.

Paper 4
J. L. Liu, A. Vosoogh, A. U. Zaman, and P. S. Kildal, "Design of 8 $\times$ 8 Slot Array Antenna based on Inverted Microstrip Gap Waveguide", in *International Symposium on Antennas and Propagation, ISAP 2016*, Okinawa, Japan, October 24-28th, 2016.

Paper 5
J. L. Liu, A. Vosoogh, A. U. Zaman, and Jian Yang, "Design and Fabrication of a High Gain 60-GHz Cavity-backed Slot Antenna Array fed by Inverted Microstrip Gap Waveguide", *IEEE Transactions on Antennas and Propagation*, vol. 65, no. 04, pp.2117-2122, April, 2017.

Paper 6
J. L. Liu, Jian Yang, and A. U. Zaman, "Analytical Solutions towards Inverted Microstrip Gap Waveguide for characteristic Impedance and Losses based on variational Method", submitted to *IEEE Transactions on Antennas and Propagation*,

Contents

II Included Papers

Part I

Introductory Chapters

Chapter 1

Introduction

Currently, considerable attention has been paid to millimeter and sub-millimeter wave communications [1]. In commercial applications, such as high-speed wireless access and high streaming multimedia transmission, millimeter wave systems are able to supply 100 times higher data than present WLAN and Wi-Fi technologies [2]. However, wireless communications at such frequency bands are easily affected by the propagation loss and strong atmospheric absorption according to fundamental principles of electromagnetic field theory [3]. Therefore, ultra-low loss materials and high gain antennas are required for such kind of wireless systems.

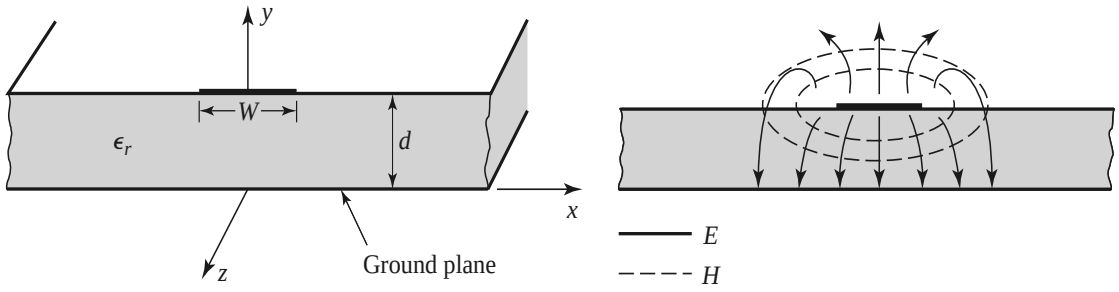

Figure 1.1: Microstrip Transmission Line.

As is well-known, transmission lines are frequently utilized for traditional communications systems. Transmission lines are specialized cable structures which carry alternate current of radio frequency. In reality, transmission lines are used with the purposes such as connected circuits for transmitter, receiver and antennas, distributed television cable and high speed bus system in a computer. The most common types of transmission lines are microstrip line and stripline. A microstrip line is the most popular transmission line, as illustrated in Figure 1.1. A good conductor which is usually copper of Width W is printed on a thin, grounded dielectric substrate of thickness

d and relative permittivity ε_r. A regular sketch of the corresponding E- and H-fields

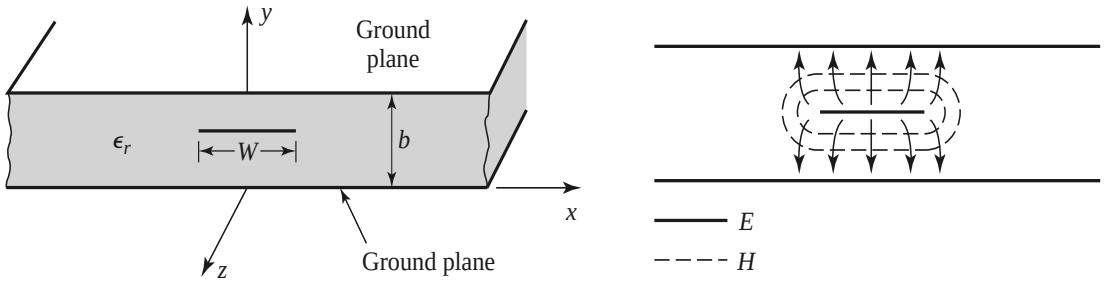

Figure 1.2: Stripline Transmission Line.

is also shown in the figure. Similarly, the geometry of a stripline transmission line is depicted in Figure 1.2. A thin conducting strip of width W is centered between two wide conducting ground planes of separation b, the area between the ground planes is filled with a dielectric material. In reality stripline is usually constructed by etching the center conductor on a grounded dielectric substrate of thickness $b/2$ and then covering with another grounded substrate.

Generally, the total loss energy in a RF system consists of dielectric loss and conducting loss. Considering that those two guiding structures suffer from dielectric substrate, the dielectric loss is unavoidable in them. The stripline and the microstrip line are typical applied topologies based on parallel-plate transmission line. Theoretically, the dielectric loss can be expressed as the multiplication of the frequency and loss tangent of the materials. Therefore, the corresponding dielectric loss squarely increases against the frequency. The high dielectric loss is the main existing problem in transmission lines at millimeter wave frequency band.

The waveguide structure usually refers to the rectangular waveguide, circular waveguide and even optical fiber. A typical geometry of rectangular waveguide is depicted in Figure 1.3. Usually, there is an obvious difference among these three structures.The key point again focuses on the dielectric substrate. The optical fiber as a main transmission component employs dielectric substrate of silicon. The pure silicon, namely glass is normally filled in it. However, rectangular and circular waveguide usually does not contain any substrate. However, the manufacture and the fabrication cost will also be considered for millimeter wave frequency band. Until now we have several methods to fabricate waveguide structures, such as Computerized Numerical Control machining and Electric Discharging Machining. Generally, the waveguide structures are typically manufactured in split-blocks and then be connected by screwing, diffusion bonding or deep-brazing techniques. In millimeter wave band the split-blocks are very small so that the manufacture outcomes usually are not accurate and perfect.

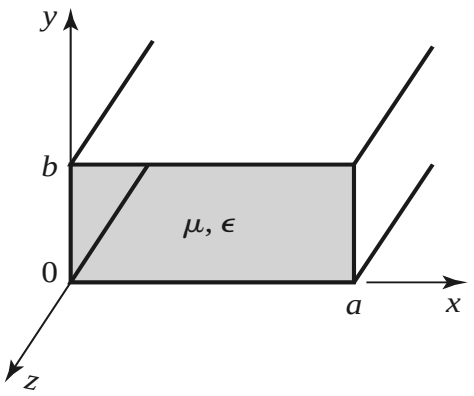

Figure 1.3: The geometry of a rectangular waveguide.

Substrate integrated waveguide (SIW) [4] has shown big advantages than both standard rectangular waveguide and printed circuit based transmission lines in millimeter waves. Geometrically, SIW is a compact planar printed circuit in which two rows of metallic via holes are embedded within a substrate material between two metallic plates, as illustrated in Figure 1.4. The electromagnetic behaviors of SIW is similar to those of rectangular waveguides with filled dielectrics. The difference existing is that the electromagnetic wave propagates between two rows of metallic via

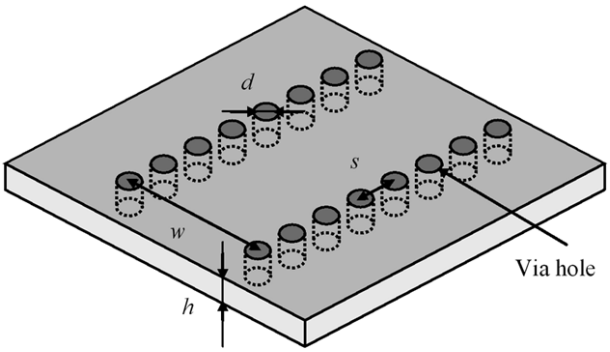

Figure 1.4: The geometry of a rectangular waveguide.

holes instead of metallic walls in rectangular waveguide. Moreover, SIW has an outstanding profile which facilities its easy integration with active RF components, such low noise amplifier, power amplifier and mixer.Nevertheless, SIW still has dielectric loss like normal microstrip lines due to the utilization of the substrate. Applying low loss substrate materials is a choice to fabricate the SIW structure, but the dielectric loss still exists and its cost might increase. Another critical point to the overall loss in SIW is the leakage energy through the gaps between metallic via holes when these are

not properly organized. Thereby, the dimensions of metallic via holes, the periodic space and the contact between two plates might increase the design complexity.

Multilayer technology [5] presents practical advantages in millimeter wave frequency band. The main advantage of multilayer technology is focusing on design of printed antenna array at millimeter wave frequency band. The multilayer technology mainly considers the transition and interconnections between several different layers, which is very practical in millimeter wave antenna arrays and integrated microwave components. Taking a simple two-layer microstrip circuit with glass Teflon substrates for both layers for example, it will be essential to take into account a proper transition technique to couple energy between transmission lines. This coupling mechanism can be achieved using different devices, depending on whether it is applied between microstrip lines or between microstrip lines and antennas. Different options can be defined as follows: coaxial transition between lines, aperture coupled patch antenna to couple energy between line and antenna and slot transition between lines with one or two outputs. According to the fundamental theory, the substrate thickness must be low compared to the wavelength in order to achieve proper efficiency for millimeter wave antennas. For instance, thickness often equals 0.1 or 0.2 mm between 30 and 100 GHz. Therefore, the printed circuits are very thin and flexible. Then, it becomes useful to apply a thick ground plane to rigidify the antenna. Additionally, this thick metallic support allows the active components to be placed more easily. For slot transition and aperture coupled patch antenna, the coupling slot will be engraved in the support. It will then be essential to take into account the fact that a thick ground plane has been added. Hence, it will be necessary to increase the slot length or to change the slot shape to permit the coupling between layers. At low frequencies (several gigahertz), a ground plane is often very thin ($\leq 0.001\lambda$). It is then possible to consider this slot as infinitely thin. On the contrary, at millimeter waves, this parameter becomes more influential. For instance, if we consider only a 0.2 mm-thick slot, it corresponds to 0.05λ at 77 GHz. The impact could be strong on the reflection coefficient and on the coupling between lines or between line and patch. Several research institutes have already achieved a great deal of outcomes in

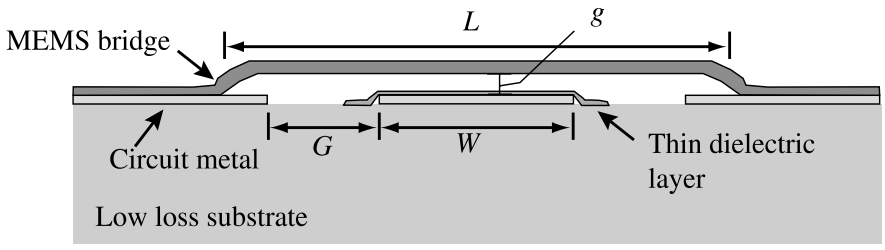

Figure 1.5: The geometry of a typical RF MEMS switch.

the fields of antenna and passive circuits. Nevertheless, due to the use of substrate the multilayer technology still face the dielectric loss.

MEMS, which is short for micro-electrical-mechanical-system, is also being development for wireless communications [6]. A typical MEMS switch geometry is illustrated in Figure 1.5. As is well-known, the simplest devices in circuits and systems, such as switches, inductors, resistors and capacitors are crucial in wireless systems because people are requiring high performance and functionality with the dimensions reducing. Thereby, these requirements in decreasing dimensions and meanwhile higher functionality consequently increase the design complexity, manufacturing cost and corresponding weight. In microwave frequency band RF MEMS is a good candidate because it enables the design of new products with good functionality, low insertion loss, high isolation and reduced power consumption. Recently, RF MEMS devices have opened up a wide range of technological approaches to enhance reconfigurable antenna systems. Furthermore, this technology might even enable new antenna concepts previously not practically usable. Particularly in terms of reduction in losses and power consumption, MEMS switches have demonstrated better performance compared with traditional ones. Up to now there are several different approaches to actuate RF MEMS switches. Magnetic, thermal, electrostatic and

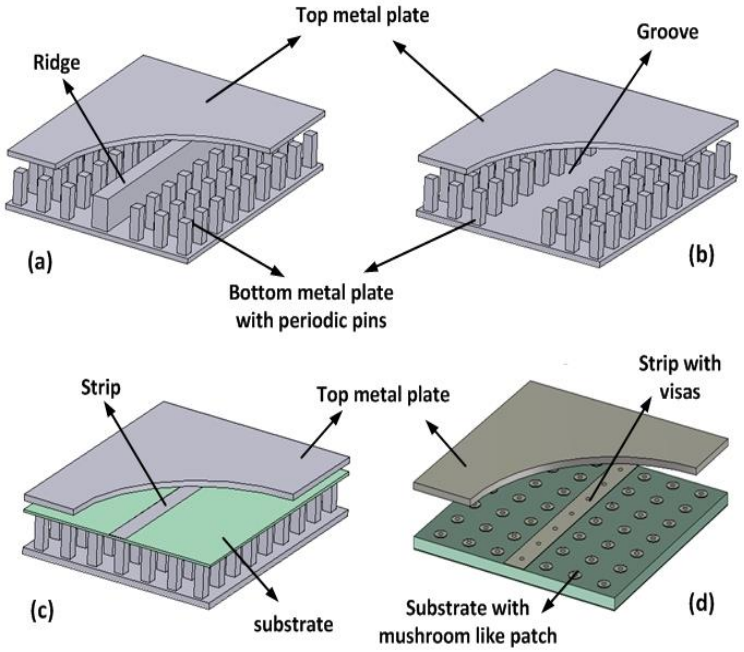

Figure 1.6: Four realized different gap waveguide geometries. (a) Ridge Gap Waveguide. (b) Groove Gap Waveguide. (c) Inverted Microstrip Gap Waveguide. (d) Microstrip-Ridged Gap Waveguide.

piezoelectric actuation methods have been applied. Among those all technologies, electrostatic actuation is the most commonly utilized approach. However, as the fre-

quency of the RF MEMS switches increasing, the dimension of corresponding device is supposed to be smaller and smaller so that the manufacturing cost rapidly increase. Compare with CMOS technology, it does not have big competitiveness at millimeter wave frequency in the fields of fabrications cost and functionality. Especially, when the dimension of RF MEMS goes into the nanometers, the so-called nano-electrical-mechanical-systems requires very high manufacturing cost.

The recently introduced gap waveguide technology [7] constitutes a new type of wave guiding structure which presents lots of potential to overcome the problems existing in conventional technologies mentioned before. The newly proposed gap waveguide technology is based on the research results of soft- and hard- surfaces [8], which states the cutoff of electromagnetic fields when a metal plate is placed parallel to a textured artificial magnetic conductor (AMC) and their distance is smaller than quarter wavelength. The AMC surface is able to establish a high impedance surface boundary condition that ensures the removal of any parallel-plate mode, cavity mode, surface waves within a certain frequency band called the stopband. Usually this AMC is realized by the periodic structure by metallic pins or mushrooms. Then only a local TEM mode is allowed to propagate confined within the air gap and along a desired path defined by a metallic ridge, groove or microstrip embedded in the AMC layer. Therefore, the gap waveguide technology is able to control the wave propagation in the desired paths, and forbids propagation of waves in undesired directions. Thereby, the gap waveguide technology is a promising wave guiding structure alternative to counteract the limitations of conventional technologies mentioned before in this report. So far there are four different realized versions based on guiding-line, propagation characteristics and the band gap structure. Ridge gap waveguide, groove gap waveguide, inverted microstrip gap waveguide and microstrip-ridge gap waveguide are four different varieties of gap waveguide technology, as depicted in Figure 1.6. Firstly, the ridge gap waveguide guides a TE mode along the metallic ridge surrounding by metallic pins and no dielectrics is required in the structure. Then the inverted microstrip gap waveguide guides a quasi-TEM mode along a microstrip etched on a Printed Circuited Broad (PCB). This PCB can be either supported by an AMC surface or AMC itself embedded in the substrate materials. In inverted microstrip gap waveguide the field is mainly confined in the air gap. The last groove gap waveguide can propagate a TE mode along the periodic pins surface. No substrate material is involved in the geometry. This cutoff principle on which this new technology is based, provides promising opportunities compared to the conventional approaches, such as microstrip, coplanar waveguide, and standard waveguides. The gap waveguide technology has interesting characteristics such as low loss, easy manufacturing, and cost-effectiveness at millimeter wave frequencies. The advantage compared with other candidates is low loss because the wave propagates in the air. Secondly, the ridge and groove gap waveguide does not contain any dielectrics so that they can totally avoid the dielectric loss. Furthermore, they are mechanically more flexible to

fabricate and assemble them than normal hollow waveguide. In addition, electrical contact between the building blocks is not needed anymore in such kinds of novel structures. Thereby, this advantage offers good opportunities for making millimeter wave antennas and corporate feed networks. And most importantly, gap waveguides geometries can be manufactured by the usage of low cost fabrication techniques such as injection molding, die pressing, plastic hot embossing or electrical discharging machining.

Another useful advantage of gap waveguide technology is that the metallic pins are able to supply PMC boundary condition. This boundary condition is able to avoid the surface current which is the origin for the metallic loss. This huge advantage can be utilized to package the integrated circuits [9] and passive elements [10]. Microstrips and coplanar waveguide transmission lines are open structures and the final products need to be protected from interference and physical damages. The traditional method is based on using metallic shielding boxes. As we discussed before, the metallic shielding boxes produce the surface current based on fundamental electromagnetic boundary condition. In addition, this method allows easy appearance of cavity resonance modes when two of the dimensions of the box are larger than half wavelength. It is possible to suppress these resonances by adding absorber materials, which introduces additional losses. The new gap waveguide technology can avoid all such problems depicted in traditional method.

1.1 Goal and outline of the thesis

In this thesis, some of issues of the traditional technologies and challenges in the millimeter wave communications in the future have been already discussed very detailed. There exists a big gap between the planar transmission lines such as microstrips, coplanar waveguide, SIW, multilayer technology, RF MEMS and traditional hollow waveguide. One of the main current research challenges is to find a new guiding structure with flexible, low cost manufacture and low loss at the same time. Taking the millimeter wave antennas design as examples, RF MEMS and hollow waveguide are able to realize a high efficiency antennas, but the manufacture cost are very high. Microstrip, SIW and multilayer technology have low cost and easy manufacture, but they suffer from high loss and low efficiency. It is very difficult to combine all advantages together at the same time. However, it is possible to utilize gap waveguide technology to cover all advantages together. In addition, gap waveguide concerns electromagnetic packaging aspects of this new approach and design of millimeter wave transitions. This technology also shows effective package advantage, particularly applied to microstrip circuits. Furthermore, in order to achieve high integration between passive components, active components and antennas together, the gap waveguide technology is able to supply good integration ability with mono-

lithic microwave integrated circuits. The transitions [11] from gap waveguide to other conventional structures has showed that it is very suitable to integrate other components. In the next chapter, the high-gain high-efficiency array antenna based on the inverted microstrip gap waveguide technology will be detailedly introduced.

Chapter 2

High Gain 60-GHz array antenna based on Gap Waveguide

This chapter deals with the design of high gain array antennas based on gap waveguide. Compared with the other technologies introduced in chapter 1, gap waveguide decreases cost and complexity of fabrication process without the strict requirement of electric contact among different layers. In this chapter a high gain array antenna based on inverted microstrip gap waveguide and ridge gap waveguide will be detailed introduced. The first designed whole structure based on inverted microstrip gap waveguide consists of radiating slots, groove gap cavity layer, distribution feeding network and a transition from standard WR-15 waveguide to inverted microstrip gap waveguide [11]. The complete antenna array is designed and fabricated using Electrical Discharging Machining (EDM) technology. The measurement shows that the antenna has 16.95% bandwidth covering 54-64 GHz frequency range. The measured gain of the antenna is more than 28 dBi with the efficiency higher than 40% covering 54-64 GHz frequency range.

2.1 Introduction

The inverted microstrip gap waveguide technology is based on the presence of a thin substrate that lies over a periodic pin pattern that composes the bed of nails. This bed of nails constitutes an AMC material and the combination with the upper metal lid prohibits any wave propagation within the air gap, also in the presence of the dielectric layer. Only local waves are allowed to propagate along strips etched on this substrate. Figure 2.1 shows the basic layout of the inverted microstrip gap waveguide. As sketched in Figure 2.1, the inverted microstrip gap waveguide technology is based on the use of a thin substrate which is applied for feeding network and lies over a periodic pin pattern. This periodic metallic pin layer constitutes an AMC surface and in combination with the upper metallic lid prohibits any wave propagation within

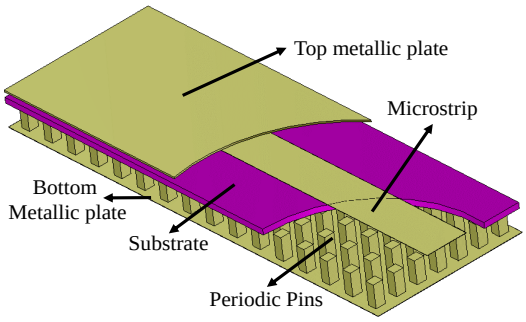

Figure 2.1: Brief geometry of the inverted microstrip gap waveguide.

the air gap. Furthermore, a local quasi-TEM mode is allowed to propagate along the metallic strip. The main motivation and advantage of this inverted microstrip gap waveguide antenna lies to the fact that the pin plate with uniform pin period can be easily fabricated by metal sawing or wire-cut technique and this will reduce the cost of the overall antenna. Also, the feeding network will be printed on a PCB which can be also low cost. In this chapter, we will systematically present a 16×16 slot antenna array designed with corporate feeding networks including an interface to WR-15 rectangular waveguide. The brief design idea of the complete 16×16 slot antenna array is shown as a flow chart in Figure 2.2.

2.2 Design for Bed of Nails

As mentioned in previous section, gap waveguide uses a parallel-plate stopband over a specific frequency range. The pin dimensions of bed of nails should be chosen correctly to achieve a parallel plate stopband which covers as much as 60-GHz frequency band. The basic idea is numerical parametric analysis of the inverted microstrip gap waveguide whose structure is illustrated in Figure 2.3. The PEC, periodic and PEC boundary conditions are added for the structure in x-, y- and z-axis, respectively. The geometrical parameters which effect the stopband of inverted microstrip gap waveguide are: the gap height h_g, the period p of pins, the width a of pins, the pin height h_p of pins and the thickness of substrate h_s. Here the shape of pins in XOY plane is square while dispersion diagrams metallic strip are supposed to be identical in the both propagation directions x and y. The starting point [12] for the parametric analysis is based on the following rules: the height of the air gap h_g must be smaller than $\lambda/4$ in order to stop the propagation of all parallel-plate modes. Secondly, the height of metallic pins h_p is supposed to be approximately equal to $\lambda/4$ so that highest surface impedance is achieved. The ratio between the width of metallic pins and period a/p has been chosen as 0.5. The considered substrate material

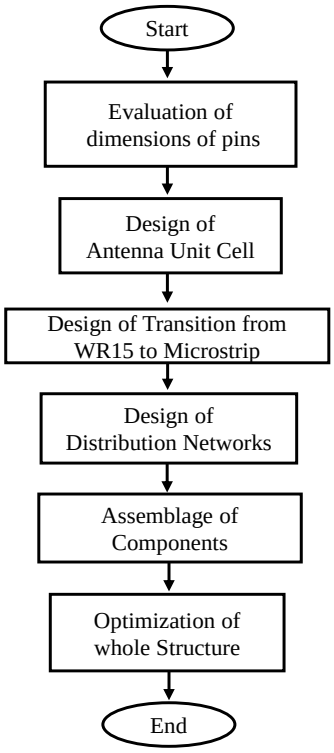

Figure 2.2: The flow chart for design the whole structure in this thesis.

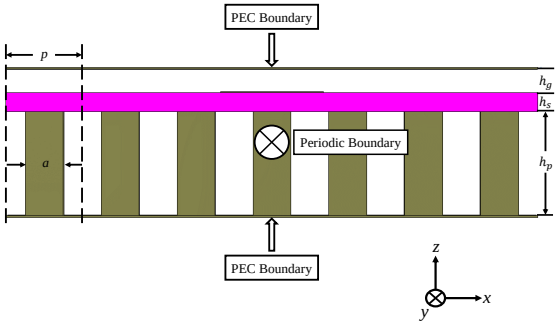

Figure 2.3: Geometrical interpretation of gap waveguide microstrip line. Along the y-axis Periodic Boundary Condition is set up and the structure is simulated in CST Microwave Studio using Eigenmode Solver.

Table 2.1: Geometrical Parameters of the Structure in Figure 2.3

	h_s	h_g	h_p	a	p
Geometrical Parameters	0.2 mm	0.25 mm	1.2 mm	0.4 mm	0.8 mm

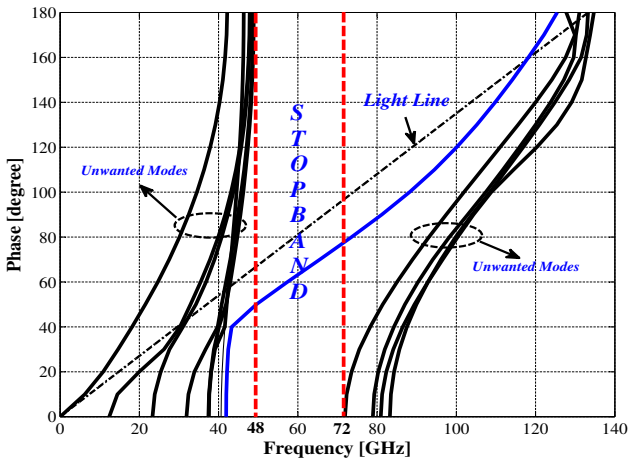

Figure 2.4: Dispersion diagram for the structure in Figure 2.2 and the blue curve crossing over the stopband represents the quasi-TEM mode.

is Rogers $RO4003$ with relative permittivity $\varepsilon_r = 3.55$, loss tangent $tan\delta = 0.0027$ (specifications are at 10 GHz according to Rogers material data sheet) and thickness $h_s = 0.2$ mm. It should be emphasized that the loss tangent value of the substrate material Rogers $RO4003$ at 60-GHz frequency band is much higher than that at 10 GHz in reality according to fundamental electromagnetic field theory. Therefore, we have to set up the loss tangent value of Rogers $RO4003$ as 0.01 in CST Microwave Studio, which is almost 4 times higher than the value at 10 GHz. The motivations to select $RO4003$ are that it has lower loss value than traditional PCB substrate $FR4$ and mechanically more rigid than other substrate materials. Correspondingly, the dispersion diagram of the structure is shown in Figure 2.4, which is obtained by utilizing the eigenmode solver in CST Microwave Studio software. The obtained stopband is from 48 to 72 GHz and only one mode propagates within the structure, as shown in Figure 2.4. The corresponding geometrical parameters are listed in Table 2.1.

2.3 Design for Antenna Unit Cell

As mentioned before, a 2×2 element sub-array is firstly designed using periodic boundary condition in order to evaluate the radiation pattern and directivity of whole array antenna. Most importantly, the mutual coupling effect is taken into account in this way so that the periodic boundary conditions in both x and y directions are placed. Figure 2.5 shows exploded perspective view of the 2×2 element sub-array, which briefly consists of radiating slot layer, cavity layer, PCB microstrip layer and bed of nails. Instead of normal hollow rectangular waveguide cavity [13], we have uti-

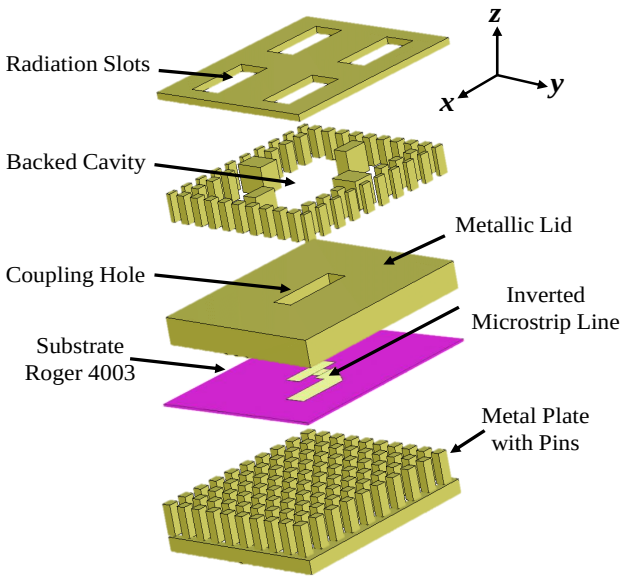

Figure 2.5: Detailed 3-D view of 2 × 2 slots sub-array.

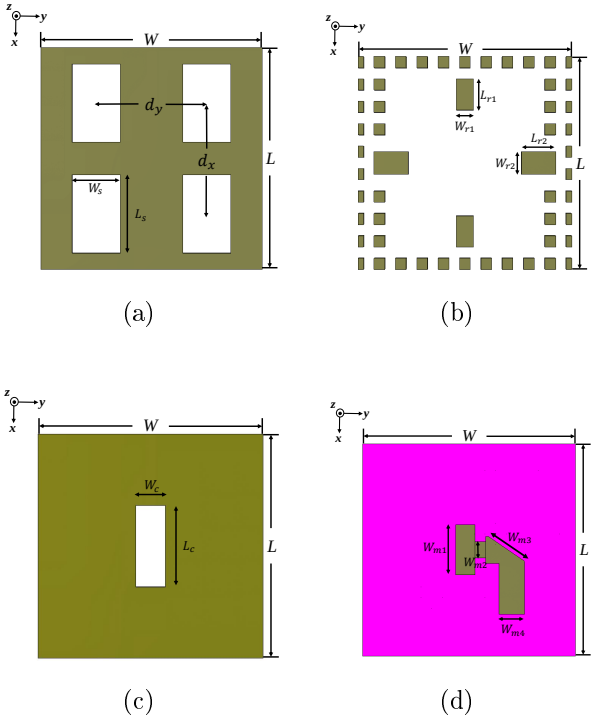

Figure 2.6: Geometrical parameters of a 2 × 2 slots array. (a) Top radiation slots layer. (b) Backed cavity layer. (c) Coupling hole layer. (d) Feed distribution networks layer.

lized groove gap waveguide cavity here because it is convenient to be manufactured. Here the groove gap waveguide cavity in the middle is partitioned into four spaces by two sets of metallic blocks extending in the x and y directions. The PCB microstrip layer feeds all the groove waveguide cavities with identical phase and amplitude by

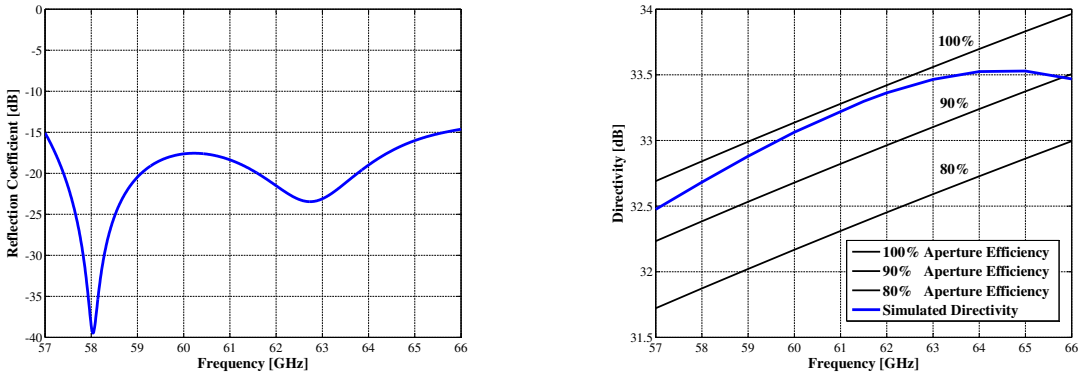

(a) (b)

Figure 2.7: (a) Simulated reflection coefficient S_{11} of 2×2 slots sub-array. (b) Directivity of an array antenna of 16×16 slot aperture dimension in infinite array environment.

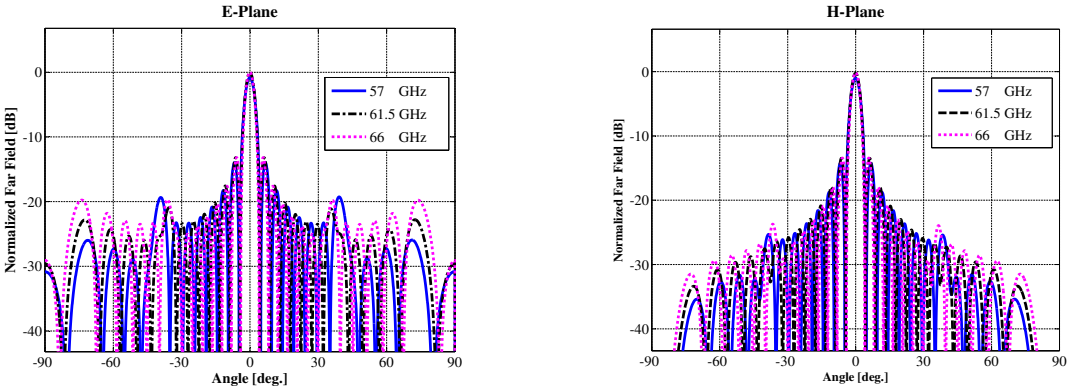

(a) (b)

Figure 2.8: (a) Radiation pattern of 16×16 slot array antenna in E-Plane. (b) Radiation pattern of 16×16 slot array antenna in H-Plane. Both simulation results are obtained by infinite periodic approach on 2×2 slot sub-array.

the middle coupling hole.

As is well known, the slots in an antenna aperture ought to be uniformly spaced in both x and y directions with spacing smaller than one wavelength in order to avoid grating lobes in a large broadside array. The highest frequency of the antenna is chosen to be 66 GHz and the corresponding wavelength λ is about 4.5 mm. Therefore,

the slot space d_s in this work we have chosen 4 mm. On the other hand, the value W and L should be integer times of the pins period, namely $W = Mp$ and $L = Np$. Given the above-mentioned considerations, we select $W = L = 10p = 8$ mm. The detailed geometrical demonstration of the antenna sub-array have been shown in Fig. 6. First of all, the slot dimensions W_s and L_s as well as the cavity metallic block dimensions W_{r1}, L_{r1}, W_{r2} and L_{r2} have been well optimized to achieve good radiation pattern. Secondly, W_c, L_c, W_{m1}, W_{m2}, W_{m3} and W_{m4} have been optimized to achieve minimum reflection coefficient. Figure 2.7 (a) shows corresponding reflection coefficient of sub-array and it has 14.5% impedance bandwidth (over 57-65.7 GHz)

Table 2.2: Geometrical Parameters of 2 × 2 Unit Cell the Structure in Figure 2.6

	W	L	d_x	d_y	W_s
Geometrical Parameters	8 mm	8 mm	4 mm	4 mm	1.75 mm
	L_s	W_c	L_c	W_{r1}	L_{r1}
Geometrical Parameters	2.832 mm	1.748 mm	2.742 mm	0.637 mm	1.111 mm

with input reflection coefficient better than -15 dB. Figure 2.7 (b) also illustrates the simulated directivity of 16×16 slot aperture array in infinite array environment. The optimized sub-array achieves that expected design target for whole antenna array. The final dimensional parameters of sub-array are presented in Table 2.2. Here we have utilized the CST Microwave Studio infinite periodic approach along the x and y directions of 8 elements in order to estimate the radiation pattern of the whole structure. Figure 2.8 illustrates the radiation patterns of E- and H-plane of 16×16 slot array antenna according to infinite periodic approach. We have observed that the first side-lobe levels in both E- and H-planes are around -13 dB and the grating lobe levels (GL) in E- and H-planes are respectively below -19 dB and -25 dB.

2.4 Transition from WR-15 to Inverted Microstrip Gap Waveguide

A vertical transition from standard V-band rectangular waveguide to inverted microstrip gap waveguide is presented in this work. Since it is convenient to directly measure antenna array with rectangular waveguide excitation, millimeter wave high gain antennas are usually excited by a standard rectangular waveguide in reality. A standard V-band rectangular waveguide (WR-15) thus works as the input port at the bottom of antenna structure. Obviously, the main challenge here is how to transfer TE_{10} mode in rectangular waveguide to the quasi-TEM mode of inverted microstrip gap waveguide efficiently with simple configureation. Normally there are three types of transitions in microwave technology: inline transitions, aperture coupled patch transitions and vertical transitions. Here we choose the vertical transition.

As sketched in Figure 2.9, this transition is composed of three parts: WR-15

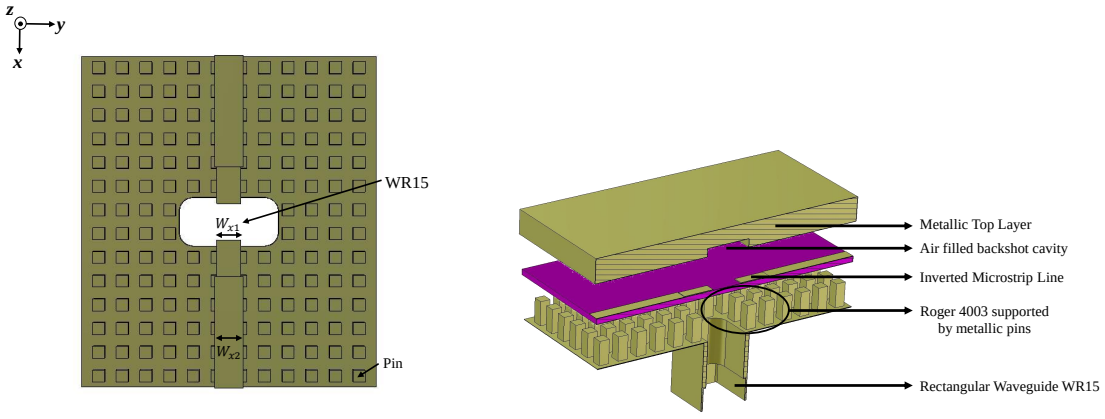

(a) (b)

Figure 2.9: (a) Top view transition geometry. In order to observe the microstrip and waveguide open details the substrate is hidden. (b) Cross-sectional view for complete structure.

feeding waveguide, inverted microstrip gap waveguide and backshort cavity at top metallic layer. The whole structure works as a three-port power divider that can be also utilized for power division. First of all, a PCB is positioned over a bed of pins and

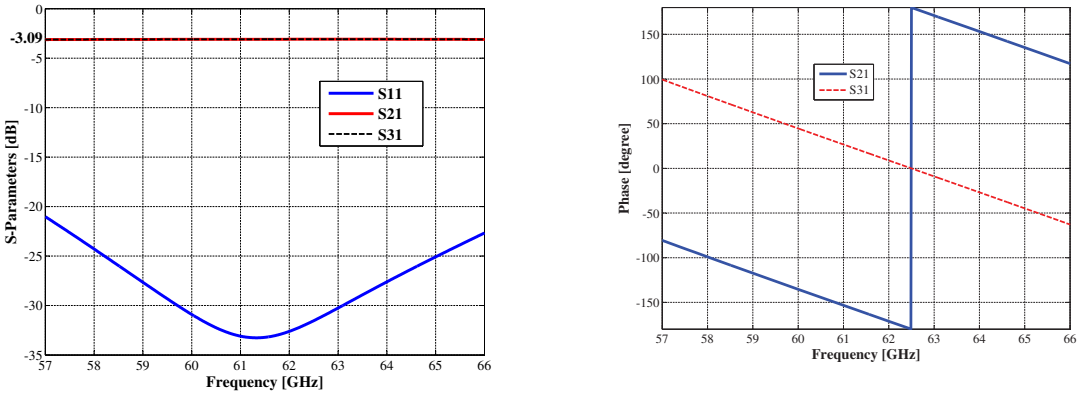

(a) (b)

Figure 2.10: Simulated S-parameter results of designed transition structure. (a) Amplitude. (b) Phase.

it contains tapered section. These tapered-line sections act as an impedance transformer. A parametric sweep of the position and impedance of this tapered section has been carried out in order to achieve optimum return loss within the frequency band of interest. The layout of the transition circuit is shown in Figure 2.9 (a). On the other hand, the whole transition is accomplished by adding a cavity backshort on the top metallic lid, as shown in Figure 2.9 (b). The backshort is positioned opposite

Table 2.3: Geometrical Parameters in Figure 2.9

	W_{x1}	W_{x2}	L_{cbx}	L_{cby}	L_{cbz}
Geometrical Parameters	0.815 mm	0.961 mm	3 mm	1.785 mm	0.375 mm

to the rectangular waveguide opening. Its dimensions are firstly roughly evaluated by impedance transformer and then optimized together with the tapered-line by full wave simulation. The distance between the backshort cavity and the substrate is set as $\lambda_0/4$ ($\lambda_0 = 4.95$ mm) in order to compensate the reactance of two-steps microstrips. Hereby, the backshort cavity together with the tapered microstrip line essentially contributes in field matching as well as impedance matching over 57 - 66 GHz. All significant parameter values are specified on Table 2.3 for this proposed transition power divider. The simulated S-Parameters of the structure is shown in Figure 2.10. The function of simple section is actually equal to a single WR-15 to inverted microstrip gap waveguide transition and a T-junction power divider. In addition, we should notice that the phases of the output ports have 180 degree difference, as shown in Figure 2.10 (b). Please observe that we will compensate this difference in design of distribution networks.

2.5 Design of Feeding Distribution Networks

Compared with groove and ridge gap waveguide structure, the feeding distribution networks based on inverted microstrip gap waveguide has some obvious advantages. First of all, the inverted microstrip gap waveguide has a uniform bed of nails while the other types of gap waveguide prototypes do not. This uniform pins make the fabrication much easier and cheaper. For instance, a uniform pins surface can be sawed with parallel saw blades, whereas nonuniform pin locations and ridges must be milled with a thin milling tool. Secondly, theories and design principles of traditional inverted microstrip technique are very maturate in the past decades so that we can directly utilize them with little modification. For these reasons, the inverted microstrip gap waveguide is attractive in feeding networks for slot antenna arrays at high frequency.

Despite its advantages, the inverted microstrip gap waveguide technology is still a challenge in design of feeding distribution networks for slots array. In [14] a planar horn array fed by inverted microstrip gap waveguide has been already expounded. Since metallic pins surface is able to supply a nearly PMC boundary condition, the distribution networks in [14] has been first designed with an ideal PMC condition instead of metallic pins structure located at the bottom of the substrate. Nevertheless, the corporate-feed networks design in this work differs from that in [14]. Most important reason is that minute quantity of electric- and magnetic fields still exist inside the metallic pins structure in reality while a quasi-TEM mode propagates along

the top microstrip. However, electric- and magnetic fields inside a PMC are both null. Therefore, assuming an ideal PMC condition to replace the metallic pins structure may introduce significant error in design of distribution networks. Until now the inverted microstrip gap waveguide technology has been merely applied for design bandpass filter [15]. Given its complexity an antenna unit cell has been accomplished without distribution networks in [16].

As introduced before, we have already designed a promising antenna unit cell which is fed by inverted microstrip gap waveguide. In this section, a new procedure for design distribution networks based on inverted microstrip gap waveguide structure will be presented. The feeding networks consists of several cascading T-junction power dividers and their impedance matching transformers between each other.

2.5.1 Design of T-junction Power Divider

Essentially a T-junction power divider is a simple three-port network that can be utilized for power division or combining. Thereby, the T-junction is a central component in distribution networks for feeding antenna array. In this work we firstly design a T-

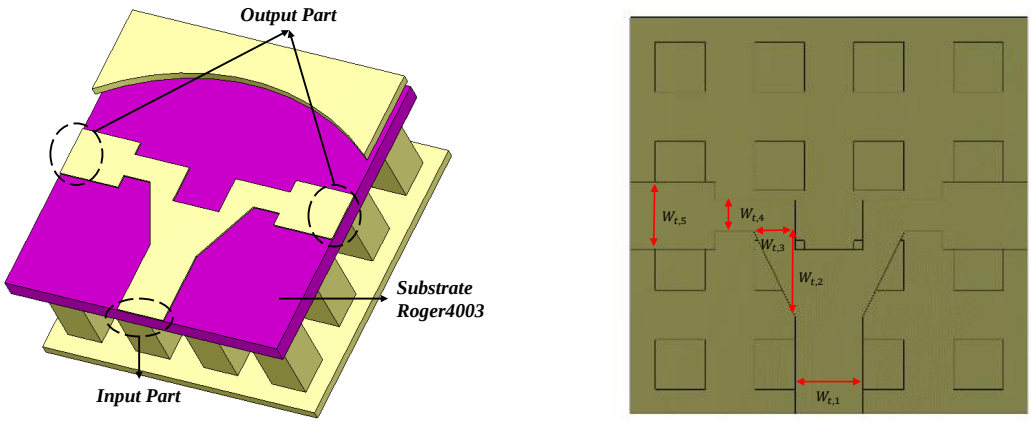

(a) (b)

Figure 2.11: (a) Illustration for single T-junction power divider based on inverted microstrip gap waveguide. (b) Geometrical description for single T-junction and the substrate is hidden in order to observe the microstrip and bottom bed of nails.

junction power divider with metallic pins in CST Microwave Studio shown in Figure 2.11 (a). In order to obtain correct transition performance an optimized numerical port [17] has been utilized during the entire design procedure. The T-junction then has been optimized with the dimensions of width of microstrips $W_{t,1}$, $W_{t,2}$, $W_{t,3}$, $W_{t,4}$ and $W_{t,5}$ and the final optimized geometrical parameters are listed in Table 2.4. Fig. 12 shows S-parameters, where the reflection coefficient S_{11} is below -30 dB from 57 to 66 GHz. The S_{21} and S_{31} are identical to -3.1 dB. Besides the lost energy in sub-

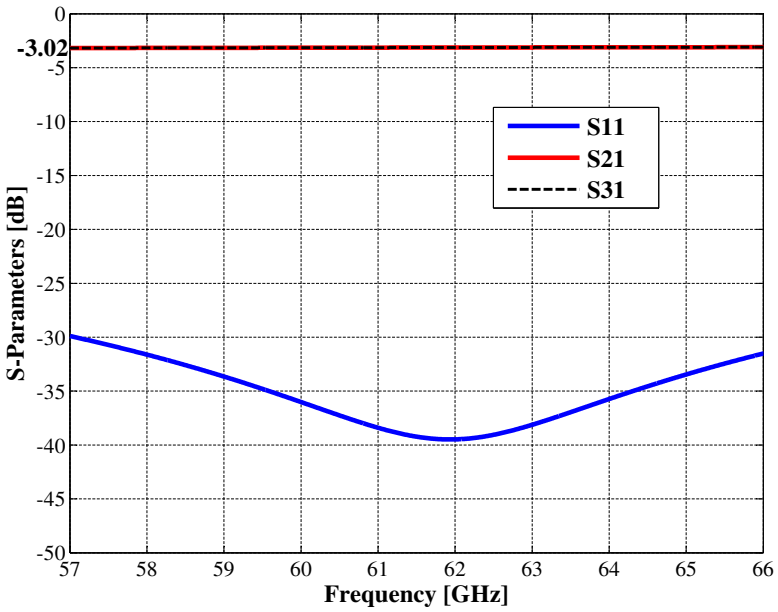

Figure 2.12: The simulated S-parameters of single T-junction.

Table 2.4: Geometrical Parameters in Figure 2.11

	$W_{t,1}$	$W_{t,2}$	$W_{t,3}$	$W_{t,4}$	$W_{t,5}$
Geometrical Parameters	1.045 mm	1.324 mm	0.306 mm	0.298 mm	1.100 mm

strate $RO4003$, the rest of electromagnetic energy are identically split to output port 2 and port 3. The simulated result also indicates that T-junction power divider has promising abilities of power division and isolation for two output ports. The input and output port impedances are calculated by CST and it is convenient to utilize them for impedance transformer design in next subsection.

2.5.2 Design of Impedance Transformer

Impedance matching is a practical topic in microwave circuits. This fundamental idea is that an impedance matching network placed between a load impedance and a transmission line. The reflection effect will be eliminated on the distribution networks to the matching networks. The basic principle of impedance matching is shown in Fig. 13 (a) and its implementation in this work is shown in Fig. 13 (b) as well. In this work we apply classical second order binomial impedance transformer for impedance matching. All characteristic impedances and load impedances has been obtained from optimized numerical ports introduced in [17]. Here we should notice

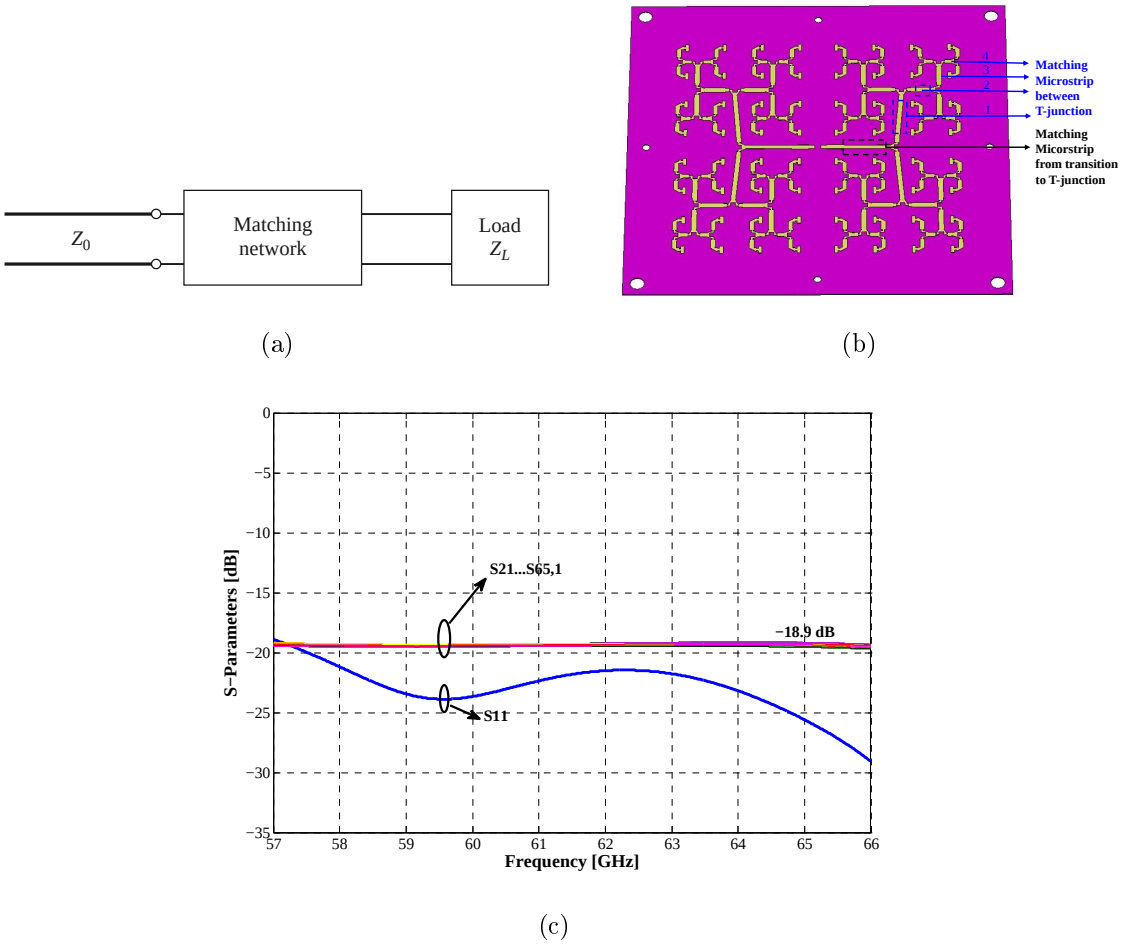

Figure 2.13: (a) Illustration for a network matching an arbitrary load impedance to a transmission line. (b) Realized whole feeding networks and its matching parts in this work. (c) Simulated S-Parameters in CST Microwave Studio.

that part 1 of matching microstrip has been designed as shape of parallelogram in order to remove its mutual coupling effect to the nearest coupling holes. In addition, the input port in CST is set up at the bottom of WR-15 and the output ports are built at the output microstrip of last stage T-junction power divider. Finally, the whole distribution network is optimized by genetic algorithm.

The final designed structure of the feeding distribution networks is shown in Fig. 13 (b). The complete corporate-feed network consists of two 32-way power dividers connected to the transition of WR-15 at the center. As described in section IV, the transition power divider from WR-15 to inverted microstrip gap waveguide has 180 degree phase difference. Thereby, the whole feeding network is mirrored in order to compensate the phase difference. Fig. 13 (c) shows the corresponding S-parameters of the whole distribution networks. The reflection coefficient S_{11} is almost below -20 dB over 57 - 66 GHz.

2.6 Comparison between Simulated and experimental results

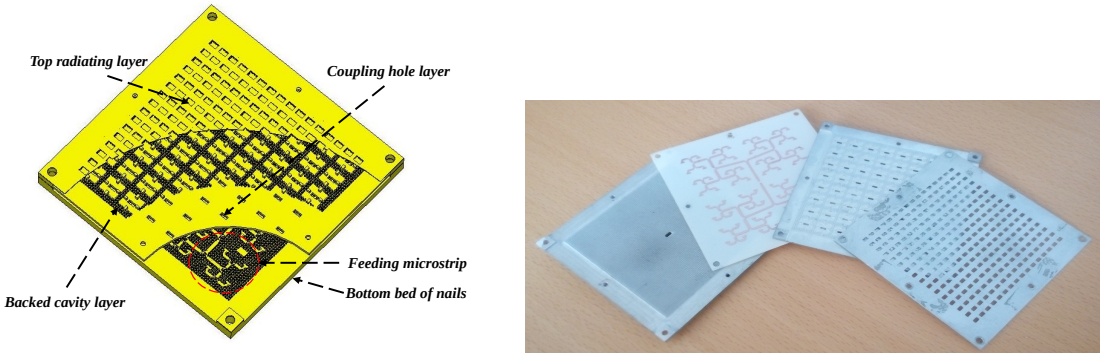

(a) (b)

Figure 2.14: (a) Numerical model in CST Microswave studio of proposed array antenna. In order to observe the microstrip and waveguide open details the substrate is hidden. (b) Photogragh of proposed 16×16 array antenna fabricated by EDM technology.

The numerical model and final manufactured prototype of the 16×16 slot array antenna discussed in this paper is shown in Fig. 14. The metallic parts of the array antenna is fabricated by Electrical Discharging Machining (EDM) Technology. In this manufacture technology, the designed prototype is etched by recurring electric discharges between the workpiece and electrodes. The final designed array aperture dimension is $64 \times 64\ mm^2$ (8 mm×8 mm× 64 elements).

The simulated and measured input reflection coefficients of the proposed antenna

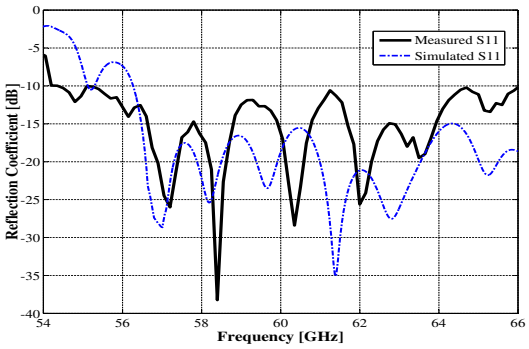

Figure 2.15: Comparison of simulated and measured reflection coefficient of the proposed 16 × 16 slot array antenna.

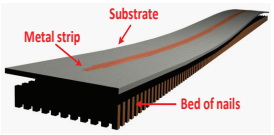

Figure 2.16: Sketch of inverted microstrip gap waveguide with a bent substrate.

are shown in Fig. 15. The measured S_{11} is a bit higher than the simulation. However, it is still below -10 dB from 54.5 GHz to 66 GHz (19.2% impedance bandwidth). There are some differences between the simulated and measured results. As above discussed in section II, the dispersion diagram of whole structure is affected by dimensions of metallic pins, the thickness of substrate and the height of air gap. Therefore, any manufacture tolerances of bed of nails and the height change of air gap will cause shift of parallel stopband. As reported in [18], there is always a frequency shift in reflection coefficient which drifts towards to lower or higher frequency. A consequence of this is that the PCB may not remain rigidly supported over the bed of pins, and there are some points in which the pins do not have a good contact with the substrate (see sketch presented in Fig. 16). Furthermore, these untouched gap between substrate and pins automatically creates capacitance effect. This small shunt capacitor affects the dispersion diagram of inverted microstrip gap waveguide.

The radiation pattern of proposed antenna is measured in an anechoic chamber. The simulated and measured normalized radiation patterns in the E- and H-plane at four different frequencies 57, 60, 61, 66 GHz are shown in Fig. 17 and Fig. 18. The measured Co-polarization radiation patterns show a very good agreement with the simulated results. The simulated and measured radiation patterns are symmetrical, and the first side-lobe levels in both E- and H-planes are around -13 dB. The measured grating lobes of the fabricated array in both E- and H-planes are below -20 dB

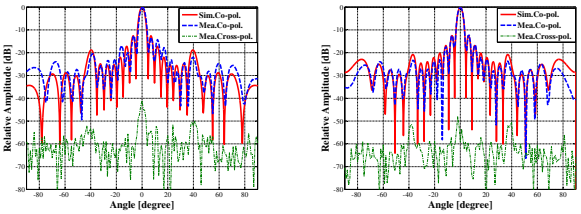

(a) (b)

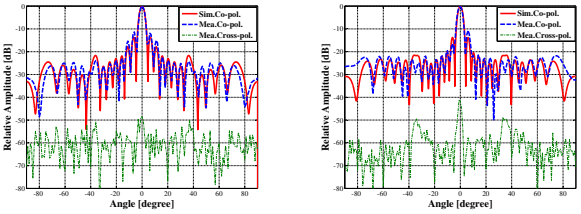

(c) (d)

Figure 2.17: Measured and simulated radiation pattern of proposed array antenna on E-plane. (a) 57 GHz. (b) 60 GHz. (c) 61 GHz. (d) 66 GHz.

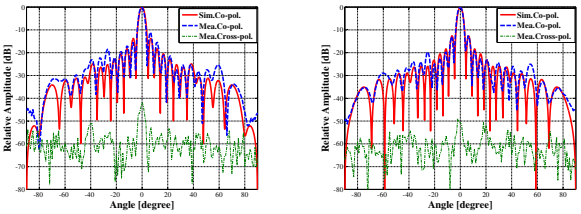

(a) (b)

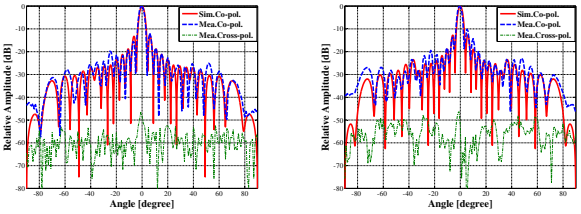

(c) (d)

Figure 2.18: Measured and simulated radiation pattern of proposed array antenna on H-plane. (a) 57 GHz. (b) 60 GHz. (c) 61 GHz. (d) 66 GHz.

over the desired frequency band. The cross-polarization values are below -40 dB at all frequencies.

The simulated directivity and gain of proposed antenna are shown in Fig. 19. The red solid line, which stand for simulated directivity, is above 80% aperture efficiency ($64\times64\ mm^2$). The pink dash line in Fig. 19 indicates the simulated gain after setting up the modified loss tangent of substrate. This method help us accurately predict the real gain after manufacturing. The blue dash-dot line in Fig. 19 shows the measured

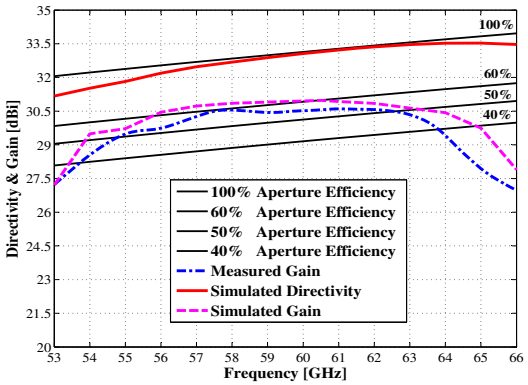

Figure 2.19: Measured gain and simulated directivity of present 16 × 16 slot array antenna.

gain, illustrating above 40% aperture efficiency over the frequency band 54-64 GHz. What we should notice in Fig. 19 is that the measured gain drops very rapidly at the start of 64 GHz, yet our design target is 57-66 GHz. The probable explanation for reducing of antenna gain of proposed array antenna is that the true loss tangent of substrate is actually unknown in reality. The value of tangent loss is probably even higher than 0.01 at higher frequency band. The other possible reason for the gain reduction is that the antenna is made of steel. The top radiating layer is too thin to be deformed by the force. The analogues phenomenons also appear in [19] and [20].

In the following we will summarize several structural characteristics and performances of reported 60-GHz high-gain antenna arrays accompanied with our work in Table 2.5. Compared with the designs in [19] and [20], our work exhibits wide impedance bandwidth, higher aperture efficiency and low cost on fabrication. However, because of the ohmic loss in dielectrics of feed distribution networks, the realized gain of our work is lower than those reported in [13], [21] and [22]. Thereby, there are still some work to do for the further improvements. As illustrated in Fig. 16, the untouched gap between pins and substrate is most important issue because it produces negative effect on wave propagation of the structure. How to solve this problem is an important issue for this technology.

Table 2.5: COMPARISON BETWEEN THE PROPOSED AND REPORTED 60-GHz PLANAR ANTENNA ARRAYS

Performance	**Ref.**[19]	**Ref.**[20]	**Present Work**
Technology	SIW/Microstrip	SIW/Microstrip	IMGW
Size [cm]	6.8 × 6.8	12 × 12	6.4 × 6.4
Number of Elements	256	256	256
Frequency Band [GHz]	57-63	58.5-64.5	54.5-64
Bandwidth	10%	10%	17%
Max Gain [dBi]	30	34	30.5
Min Efficiency	47%	25%	40%

2.7 Conclusion

A high gain and wide bandwidth slot array antenna based on inverted microstrip gap waveguide at 60-GHz has been presented in this work. The proposed antenna consists of four unconnected layers without any electric contact between them. The designed prototype is manufactured by EDM technology. In this paper, we firstly used we used a new corporate feed network based on the inverted microstrip gap waveguide technology. A transition power divider between WR-15 and inverted microstrip gap waveguide have been designed in order to provide a simple excitation of the antenna. The simulated and measured results of the whole antenna structure shows very good agreements in radiation patterns in both E- and H-plane. The measured realized gain is higher than 29 dBi over the entire operation bandwidth from 54.5 to 64 GHz, corresponding to efficiency larger than 45%. This work shows that the inverted microstrip gap waveguide technology is an excellent candidate for array antennas in millimeter wave communication.

Chapter 3

Future Work

A single layer high gain high efficiency array antenna based on ridge gap waveguide will be designed in the coming years. As is well known, millimeter wave array introduced before are all based on three layers, namely slot array layer, backed cavity layer and feed networks layer. Obviously the manufacture price is lower if we only have feed networks and slot array. At the same time this new topology still preserve the properties of high gain, high efficiency, promising radiation pattern and wide bandwidth. Secondly, bandpass filters and diplexers based on ridge gap waveguide will be developed in the future work. In addition, the package technology of active components by gap waveguide technology will also be researched in the future work.

References

[1] P. Smulders, "Exploiting the 60 ghz band for local wireless multimedia access: Prospects and future directions," *IEEE Communications Magazine*, vol. 40, no. 1, pp. 140–147, 2002.

[2] H. Song, X. Fang, and Y. Fang, "Millimeter-wave network architectures for future high-speed railway communications: Challenges and solutions," *IEEE Wireless Communications*, vol. 23, no. 6, pp. 114–122, 2016.

[3] L. Lin and Z. Li, "Study of transmission effects of millimeter wave through fog and haze," in *2016 IEEE Advanced Information Management, Communicates, Electronic and Automation Control Conference (IMCEC)*. IEEE, 2016, pp. 1591–1596.

[4] D. Deslandes and K. Wu, "Integrated microstrip and rectangular waveguide in planar form," *IEEE Microwave and Wireless Components Letters*, vol. 11, no. 2, pp. 68–70, 2001.

[5] T. Shimoto, K. Matsui, K. Kikuchi, Y. Shimada, and K. Utsumi, "New high-density multilayer technology on pcb," *IEEE Transactions on Advanced Packaging*, vol. 22, no. 2, pp. 116–122, 1999.

[6] B. Lakshminarayanan, D. Mercier, and G. M. Rebeiz, "High-reliability miniature rf-mems switched capacitors," *IEEE Transactions on Microwave Theory and Techniques*, vol. 56, no. 4, pp. 971–981, 2008.

[7] P.-S. Kildal, E. Alfonso, A. Valero-Nogueira, and E. Rajo-Iglesias, "Local metamaterial-based waveguides in gaps between parallel metal plates," *IEEE Antennas and Wireless Propagation Letters*, vol. 8, pp. 84–87, 2009.

[8] P.-S. Kildal, "Artificially soft and hard surfaces in electromagnetics," *IEEE Transactions on Antennas and Propagation*, vol. 38, no. 10, pp. 1537–1544, 1990.

[9] A. U. Zaman, M. Alexanderson, T. Vukusic, and P.-S. Kildal, "Gap waveguide pmc packaging for improved isolation of circuit components in high-frequency microwave modules," *IEEE Transactions on Components, Packaging and Manufacturing Technology*, vol. 4, no. 1, pp. 16–25, 2014.

[10] A. U. Zaman, P. Kildal, and A. A. Kishk, "Narrow-band microwave filter using high-q groove gap waveguide resonators with manufacturing flexibility and no sidewalls," *IEEE Transactions on Components, Packaging and Manufacturing Technology*, vol. 2, no. 11, pp. 1882–1889, 2012.

[11] J. Liu, A. U. Zaman, and P.-S. Kildal, "Design of transition from wr-15 to inverted microstrip gap waveguide," in *2016 Global Symposium on Millimeter Waves (GSMM) & ESA Workshop on Millimetre-Wave Technology and Applications*. [Piscataway, NJ] and [Piscataway, NJ]: IEEE, 2016, pp. 1–4.

[12] E. Rajo-Iglesias and P.-S. Kildal, "Numerical studies of bandwidth of parallel-plate cut-off realised by a bed of nails, corrugations and mushroom-type electromagnetic bandgap for use in gap waveguides," *IET Microwaves, Antennas & Propagation*, vol. 5, no. 3, p. 282, 2011.

[13] Y. Miura, J. Hirokawa, M. Ando, Y. Shibuya, and G. Yoshida, "Double-layer full-corporate-feed hollow-waveguide slot array antenna in the 60-ghz band," *IEEE Transactions on Antennas and Propagation*, vol. 59, no. 8, pp. 2844–2851, 2011.

[14] E. Pucci, E. Rajo-Iglesias, J.-L. Vazquez-Roy, and P.-S. Kildal, "Planar dual-mode horn array with corporate-feed network in inverted microstrip gap waveguide," *IEEE Transactions on Antennas and Propagation*, vol. 62, no. 7, pp. 3534–3542, 2014.

[15] A. Vosoogh, A. A. Brazalez, and P.-S. Kildal, "A v-band inverted microstrip gap waveguide end-coupled bandpass filter," *IEEE Microwave and Wireless Components Letters*, vol. 26, no. 4, pp. 261–263, 2016.

[16] S. A. Razavi, P.-S. Kildal, L. Xiang, H. Chen, and E. Alfonso, "Design of 60ghz planar array antennas using pcb-based microstrip-ridge gap waveguide and siw," in *8th European Conference on Antennas and Propagation (EuCAP), 2014*. Piscataway, NJ and Piscataway, NJ: IEEE, 2014, pp. 1825–1828.

[17] J. Liu, A. U. Zaman, and P.-S. Kildal, "Optimizing the numerical port for inverted microstrip gap waveguide in full-wave simulators," in *2016 10th European Conference on Antennas and Propagation (EuCAP)*. [Piscataway, New Jersey]: IEEE, 2016, pp. 1–5.

[18] A. A. Brazalez, E. Rajo-Iglesias, J. L. Vazquez-Roy, A. Vosoogh, and P.-S. Kildal, "Design and validation of microstrip gap waveguides and their transitions to rectangular waveguide, for millimeter-wave applications," *IEEE Transactions on Microwave Theory and Techniques*, vol. 63, no. 12, pp. 4035–4050, 2015.

[19] Y. Li and K.-M. Luk, "60-ghz substrate integrated waveguide fed cavity-backed aperture-coupled microstrip patch antenna arrays," *IEEE Transactions on Antennas and Propagation*, vol. 63, no. 3, pp. 1075–1085, 2015.

[20] J. Wu, Y. J. Cheng, and Y. Fan, "A wideband high-gain high-efficiency hybrid integrated plate array antenna for v-band inter-satellite links," *IEEE Transactions on Antennas and Propagation*, vol. 63, no. 4, pp. 1225–1233, 2015.

[21] D. Zarifi, A. Farahbakhsh, A. U. Zaman, and P.-S. Kildal, "Design and fabrication of a high-gain 60-ghz corrugated slot antenna array with ridge gap waveguide distribution layer," *IEEE Transactions on Antennas and Propagation*, vol. 64, no. 7, pp. 2905–2913, 2016.

[22] A. Vosoogh, P.-S. Kildal, and V. Vassilev, "Wideband and high-gain corporate-fed gap waveguide slot array antenna with etsi class ii radiation pattern in v -band," *IEEE Transactions on Antennas and Propagation*, vol. 65, no. 4, pp. 1823–1831, 2017.